

COMBINED INFLUENCE OF SORET AND DUFOUR EFFECTS ON NON-DARCY MIXED CONVECTIVE HEAT AND MASS TRANSFER FLOW OF A CHEMICALLY REACTING VISCOUS FLUID IN A VERTICAL CHANNEL WITH THERMAL RADIATION AND HEAT SOURCES WITH CONSTANT HEAT AND MASS FLUX

T. SIVA NAGESWARA RAO*¹, S. SIVAIAH²

**¹Research Scholar, Department of mathematics (PP. MAT. 0266),
Rayalaseema University, Kurnool, A.P, India.**

**²Professor of Mathematics, Dept. of H & S, School of Engineering & Technology,
Gurunanak Institutions Technical Campus, Ibrahimpatnam-501506,
Ranga Reddy (Dist) AP, India.**

(Received On: 03-04-17; Revised & Accepted On: 20-04-17)

ABSTRACT

In this paper we analyse the combined influence of soret and dufour effects on non-Darcy convective heat and mass transfer flow of a viscous, chemically reacting fluid in a vertical channel with heat sources. By using finite element technique the governing equations have been solved with quadratic approximation functions. The effect of various governing parameters on velocity, temperature, concentration and rate of heat and mass transfer has been discussed through graphical representations.

Key Words: Heat and Mass transfer, Vertical channel, Soret and Dufour effects, Chemical reaction, Heat sources and radiation.

1. INTRODUCTION

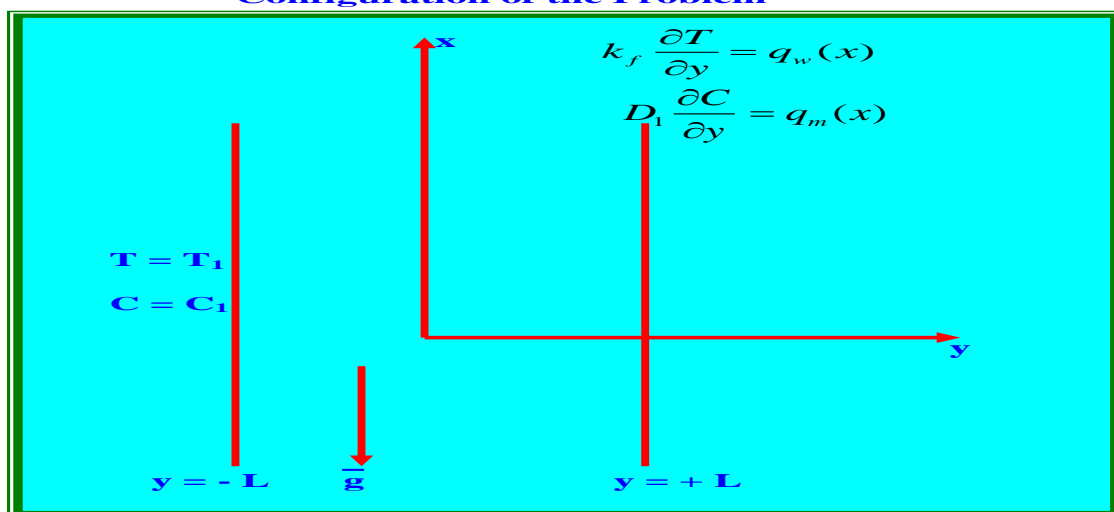
Non – Darcy effects on natural convection in porous media have received a great deal of attention in recent years because of the experiments conducted with several combinations of solids and fluids covering wide ranges of governing parameters which indicate that the experimental data for systems other than glass water at low Rayleigh numbers, do not agree with theoretical predictions based on the Darcy flow model. This divergence in the heat transfer results has been reviewed in detail in Cheng [1] and Prasad *et al.* [2] among others. Extensive effects are thus being made to include the inertia and viscous diffusion terms in the flow equations and to examine their effects in order to develop a reasonable accurate mathematical model for convective transport in porous media. The work of Vafai and Tien [3] was one of the early attempts to account for the boundary and inertia effects in the momentum equation for a porous medium. They found that the momentum boundary layer thickness is of order of $\sqrt{\frac{k}{s}}$. Vafai and Thiyagaraja

[4] presented analytical solutions for the velocity and temperature fields for the interface region using the Brinkman Forchheimer –extended Darcy equation. Detailed accounts of the recent efforts on non-Darcy convection have been recently reported in Tien and Hong [5], Cheng [1], Prasad *et al.* [6], and Kladias and Prasad [7]. Here, we will restrict our discussion to the vertical cavity only. Poulikakos and Bejan [8] investigated the inertia effects through the inclusion of Forchheimer's velocity squared term, and presented the boundary layer analysis for tall cavities. They also obtained numerical results for a few cases in order to verify the accuracy of their boundary layer analysis for tall cavities. They also obtained numerical results for a few cases in order to verify the accuracy of their boundary layer solutions. Later, Prasad and Tuntomo [2] reported an extensive numerical work for a wide range of parameters, and demonstrated that effects of Prandtl number remain almost unaltered while the dependence on the modified Grashof number, Gr, changes significantly with an increase in the Forchheimer number. This result in reversal of flow regimes from boundary layer to asymptotic to conduction as the contribution of the inertia term increases in comparison with that of the boundary term. They also reported a criterion for the Darcy flow limit. The Brinkman – Extended – Darcy modal was considered in Tong and Subramanian [9], and Lauriat and Prasad [10] to examine the boundary effects on free convection in a vertical cavity. While Tong and Subramanian performed a Weber – type boundary layer analysis,

Corresponding Author: T. Siva Nageswara Rao*¹, ¹Research Scholar, Department of mathematics (PP. MAT. 0266), Rayalaseema University, Kurnool, A.P, India.

Lauriat and Prasad solved the problem numerically for $A=1$ and 5 . It was shown that for a fixed modified Rayleigh number, Ra , the Nusselt number; decrease with an increase in the Darcy number; the reduction being larger at higher values of Ra . A scale analysis as well as the computational data also showed that the transport term $(\mathbf{v} \cdot \nabla)\mathbf{v}$, is of low order of magnitude compared to the diffusion plus buoyancy terms [7]. A numerical study based on the Forchheimer-Brinkman-Extended Darcy equation of motion has also been reported recently by Beckerman *et al.* [11]. They demonstrated that the inclusion of both the inertia and boundary effects is important for convection in a rectangular packed – sphere cavity. Also in all the above studies the thermal diffusion effect (known as Soret effect) has been neglected. This assumption is true when the concentration level is very low. Therefore, so ever, exceptions. The thermal diffusion effects for instance, has been utilized for isotropic separation and in mixtures between gases with very light molecular weight (H_2, He) and the medium molecular weight (N_2 , air) the diffusion – thermo effects was found to be of a magnitude just it can not be neglected [12]. In view of the importance of this diffusion – thermo effect, recently Jha and singh [13] studied the free convection and mass transfer flow in an infinite vertical plate moving impulsively in its own plane taking into account the Soret effect. Kafousias [14] studied the MHD free convection and mass transfer flow taking into account Soret effect. The analytical studies of Jha and singh and Kafousias [13, 14] were based on Laplace transform technique. Abdul Sattar and Alam [15] have considered an unsteady convection and mass transfer flow of viscous incompressible and electrically conducting fluid past a moving infinite vertical porous plate taking into the thermal diffusion effects. Similarity equations of the momentum energy and concentration equations are derived by introducing a time dependent length scale. Malsetty *et al.* [16] have studied the effect of both the soret coefficient and Dufour coefficient on the double diffusive convective with compensating horizontal thermal and solutal gradients. The effects of radiation on MHD flow and heat transfer problem have become more important industrially. Many processes in engineering areas occur at high temperature, and knowledge of radiation heat transfer becomes very important for the design of the pertinent equipment. Nuclear power plants, Gas turbines and various propulsion devices, for aircraft, missiles, satellites and space vehicles are examples of such engineering areas. Bharathi[17] has studied thermo-diffusion effect on unsteady convective Heat and Mass transfer flow of a viscous fluid through a porous medium in vertical channel. Radiative flow plays a vital role in many industrial and environmental process e.g. heating and cooling chambers, fossil fuel combustion energy process, evaporation form larger open water reservoirs, astrophysical flows, solar power technology and space vehicle re-entry. Taneja *et al.* [18] studied the effects of magnetic field on free convective flow through porous medium with radiation and variable permeability in the slip flow regime. Kumar et al [19] studied the effect of MHD free convection flow of viscous fluid past a porous vertical plate through non homogeneous porous medium with radiations and temperature gradient dependent heat source in slip flow regime. The effect of free convection flow with thermal radiation and mass transfer past a moving vertical porous plate was studied by Makinde [20]. Ayani *et al.* [21] studied the effect of radiation on the laminar natural convection induced by a line source. Raphil [22] have discussed the effect of radiation and free convection flow through porous medium. MHD oscillating flow on free convection radiation through porous medium with constant suction velocity w_s was investigated by El.Hakiem [22]. Nagaleelakumari[23] has studied the convective heat and mass transfer on non-darcy flow of a viscous fluid through a porous medium in a vertical channel in the presence of heat generating sources. Muralidhar [24] has analysed the thermo-diffusion effect of non-darcy convective heat and mass transfer flow in a vertical channel.

Configuration of the Problem



2. FORMULATION OF THE PROBLEM

We consider a fully developed laminar convective heat and mass transfer flow of a viscous, electrically conducting fluid through a porous medium confined in a vertical channel bounded by flat walls. We choose a Cartesian co-ordinate system $O(x, y, z)$ with x -axis in the vertical direction and y -axis normal to the walls. The walls are taken at $y = \pm L$.

The walls are maintained at constant temperature and concentration. The temperature gradient in the flow field is sufficient to cause natural convection in the flow field. A constant axial pressure gradient is also imposed so that this resultant flow is a mixed convection flow. The porous medium is assumed to be isotropic and homogeneous with constant porosity and effective thermal diffusivity. The thermo physical properties of porous matrix are also assumed to be constant and Boussinesq's approximation is invoked by confining the density variation to the buoyancy term. In the absence of any extraneous force flow is unidirectional along the x-axis which is assumed to be infinite.

The Brinkman-Forchheimer-extended Darcy equation which account for boundary inertia effects in the momentum equation is used to obtain the velocity field. Based on the above assumptions the governing equations in the vector form are

$$\nabla \cdot \bar{q} = 0 \quad (\text{Equation of continuity}) \quad (2.1)$$

$$\frac{\rho}{\delta} \frac{\partial \bar{q}}{\partial t} + \frac{\rho}{\delta^2} (\bar{q} \cdot \nabla) \bar{q} = -\nabla p + \rho g - \frac{\rho F}{\sqrt{k}} \bar{q} \cdot \bar{q} + \mu \nabla^2 \bar{q} + \mu_e J_x H - \frac{\mu}{k} \bar{q} \quad (2.2)$$

(Equation of linear momentum)

$$\rho C_p \left(\frac{\partial T}{\partial t} + (\bar{q} \cdot \nabla) T \right) = k_f \nabla^2 T + k_{22} \nabla^2 C + Q_1' (C - C_e) + Q (T - T_e) - \frac{\partial(q_R)}{\partial y} \quad (2.3)$$

(Equation of energy)

$$\frac{\partial C}{\partial t} + (\bar{q} \cdot \nabla) C = D_1 \nabla^2 C - k_1 C + k_{11} \nabla^2 T \quad (\text{Equation of diffusion}) \quad (2.4)$$

$$\rho - \rho_0 = -\beta \rho_0 (T - T_0) - \beta^* \rho_0 (C - C_0) \quad (\text{Equation of State}) \quad (2.5)$$

where $\bar{q} = (u, 0, 0)$ is the velocity, T, C are the temperature and Concentration, p is the pressure, ρ is the density of the fluid, C_p is the specific heat at constant pressure, μ is the coefficient of viscosity, k is the permeability of the porous medium, δ is the porosity of the medium, β is the coefficient of thermal expansion, k_f is the coefficient of thermal conductivity, F is a function that depends on the Reynolds number and the microstructure of porous medium, β^* is the volumetric coefficient of expansion with mass fraction concentration, k is the chemical reaction coefficient and D_1 is the chemical molecular diffusivity, q_R is the radiative heat flux, k_{11} is the cross diffusivity and Q is the strength of the heat generating source. Here the thermo physical properties of the solid and fluid have been assumed to be constant except for the density variation in the body force term (Boussinesq's approximation) and the solid particles and the fluid is considered to be in the thermal equilibrium).

Since the flow is unidirectional, the continuity of equation (2.1) reduces to

$$\frac{\partial u}{\partial x} = 0 \quad \text{where } u \text{ is the axial velocity implies } u = u(y)$$

The momentum, energy and diffusion equations in the scalar form reduces to

$$-\frac{\partial p}{\partial x} + \left(\frac{\mu}{\delta} \right) \frac{\partial^2 u}{\partial y^2} - \frac{\rho \delta F}{\sqrt{k}} u^2 - \rho g - \left(\frac{\mu}{k} \right) u - \left(\frac{\sigma \mu_e H_o^2}{\rho} \right) u = 0 \quad (2.6)$$

$$\rho_0 C_p u \frac{\partial T}{\partial x} = k_f \frac{\partial^2 T}{\partial y^2} + k_{12} \frac{\partial^2 C}{\partial y^2} + Q (T - T_e) - \frac{\partial(q_R)}{\partial y} \quad (2.7)$$

$$u \frac{\partial C}{\partial x} = D_1 \frac{\partial^2 C}{\partial y^2} - k_1 C + k_{11} \frac{\partial^2 T}{\partial y^2} \quad (2.8)$$

The boundary conditions are

$$\begin{aligned} u = 0, \quad T = T_1, \quad C = C_1 \quad \text{on } y = -L \\ u = 0, \quad k_f \frac{\partial T}{\partial y} = q_w(x), \quad D_1 \frac{\partial C}{\partial y} = q_m(x) \quad \text{on } y = +L \end{aligned} \quad (2.9)$$

The axial temperature and concentration gradients $\frac{\partial T}{\partial x}$ & $\frac{\partial C}{\partial x}$ are assumed to be constant, say, A&B respectively.

Invoking Rosseland approximation for radiation (2.9a)

$$q_r = \frac{4\sigma^*}{3\beta_R} \frac{\partial T'^4}{\partial y}$$

Expanding T^4 in Taylor's series about T_e and neglecting higher order terms

$$T'^4 \cong 4T_e^3 T - 3T_e^4 \quad (2.9b)$$

We define the following non-dimensional variables as

$$u' = \frac{u}{(\nu/L)}, (x', y') = (x, y)/L, \quad p' = \frac{p\delta}{(\rho\nu^2/L^2)}, T = T_1 + \frac{q_w(x)}{k_f}\theta, C = C_1 + \frac{q_m(x)}{D_1}C' \quad (2.12)$$

Introducing these non-dimensional variables the governing equations in the dimensionless form reduce to (on dropping the dashes)

$$\frac{d^2 u}{dy^2} = \pi + \delta(M_1^2)u - \delta G(\theta + NC) - \delta^2 \Delta u^2 \quad (2.13)$$

$$(1 + \frac{4}{3N_1})\frac{d^2 \theta}{dy^2} - \alpha\theta = (PN_T)u - Du\frac{d^2 C}{dy^2} \quad (2.14)$$

$$\frac{d^2 C}{dy^2} - (\gamma Sc)C = (Sc N_C)u + \frac{ScSo}{N}\frac{d^2 \theta}{dy^2} \quad (2.15)$$

where

$$\Delta = FD^{-1/2} \text{ (Inertia or Forchheimer parameter)} \quad G = \frac{\beta g(T_1 - T_2)L^3}{\nu^2} \text{ (Grashof Number)}$$

$$D^{-1} = \frac{L^2}{k} \text{ (Darcy parameter)} \quad Sc = \frac{\nu}{D_1} \text{ (Schmidt number)} \quad N = \frac{\beta^*(C_1 - C_2)}{\beta(T_1 - T_2)} \text{ (Buoyancy ratio)}$$

$$P = \frac{\mu C_p}{k_f} \text{ (Prandtl Number)} \quad \gamma = \frac{k_1 L^2}{D_1} \text{ (Chemical reaction parameter)}$$

$$N_T = \frac{AL}{(T_1 - T_2)} \text{ (Non-dimensional temperature gradient)}$$

$$N_c = \frac{BL}{(C_1 - C_2)} \text{ (Non-dimensional concentration gradient)} \quad S_0 = \frac{k_{11}\Delta T}{\nu \Delta C} \text{ (Soret parameter)}$$

$$Du = \frac{k_{12}\Delta C}{k_f \Delta T} \text{ (Dufour parameter)} \quad N_1 = \frac{\beta_R k_f}{4\sigma^* T_e^3} \text{ (Radiation parameter)}$$

$$N_2 = \frac{3N_1}{4 + 3N_1}, \quad P_1 = PN_2, \alpha_1 = \alpha N_2 \quad M_1^2 = M^2 + D^{-1}$$

The corresponding boundary conditions are

$$\begin{aligned} u = 0, \quad \theta = 0, \quad C = 0 \quad \text{on } y = -1 \\ u = 0, \quad \theta' = 1, \quad C' = 1 \quad \text{on } y = +1 \end{aligned} \quad (2.16)$$

3. FINITE ELEMENT ANALYSIS

To solve these differential equations with the corresponding boundary conditions, we assume if u^i, θ^i, c^i are the approximations of u, θ and C we define the errors (residual) E_u^i, E_θ^i, E_c^i as

$$E_u^i = \frac{d}{d\eta} \left(\frac{du^i}{d\eta} \right) - M_1^2 u^i + \delta^2 A(u^i)^2 - \delta G(\theta^i + NC^i) \quad (3.1)$$

$$E_c^i = \frac{d}{dy} \left(\frac{dC^i}{dy} \right) - (\gamma Sc)C^i + \frac{ScSo}{N} \frac{d}{dy} \left(\frac{d\theta^i}{dy} \right) - Sc N_c u^i \quad (3.2)$$

$$E_\theta^i = \frac{d}{dy} \left(\frac{d\theta^i}{dy} \right) - P_1 N_T u^i + Du N_2 \frac{d}{dy} \left(\frac{dC^i}{dy} \right) - \alpha_1 \theta^i \quad (3.3)$$

where

$$\left. \begin{aligned} u^i &= \sum_{k=1}^3 u_k \psi_k \\ C^i &= \sum_{k=1}^3 C_k \psi_k \\ \theta^i &= \sum_{k=1}^3 \theta_k \psi_k \end{aligned} \right\} \quad (3.4)$$

These errors are orthogonal to the weight function over the domain of e^i under Galerkin finite element technique we choose the approximation functions as the weight function. Multiply both sides of the equations (3.1 – 3.3) by the weight function i.e. each of the approximation function ψ_j^i and integrate over the typical three noded linear element (η_e, η_{e+1}) we obtain

$$\int_{\eta_e}^{\eta_{e+1}} E_u^i \psi_j^i dy = 0 \quad (i = 1, 2, 3, 4,) \quad (3.5)$$

$$\int_{\eta_e}^{\eta_{e+1}} E_c^i \psi_j^i dy = 0 \quad (i = 1, 2, 3, 4,) \quad (3.6)$$

$$\int_{\eta_e}^{\eta_{e+1}} E_\theta^i \psi_j^i dy = 0 \quad (i = 1, 2, 3, 4,) \quad (3.7)$$

where

$$\int_{\eta_e}^{\eta_{e+1}} \left(\frac{d}{d\eta} \left(\frac{du^i}{d\eta} \right) - M_1^2 u^i + \delta^2 A (u^i)^2 - \delta G (\theta^i + NC^i) \right) \psi_j^i dy = 0 \quad (3.8)$$

$$\int_{\eta_e}^{\eta_{e+1}} \left(\frac{d}{dy} \left(\frac{dC^i}{dy} \right) - \gamma C^i + \frac{ScSo}{N} \frac{d}{dy} \left(\frac{d\theta^i}{dy} \right) - ScN_c u^i \right) \psi_j^i dy = 0 \quad (3.9)$$

$$\int_{\eta_e}^{\eta_{e+1}} \left(\frac{d}{dy} \left(\frac{d\theta^i}{dy} \right) - P_1 N_T u^i + Du \frac{d}{dy} \left(\frac{d}{dy} \right) \left(\frac{d\theta^i}{dy} \right) - \alpha \theta^i \right) \psi_j^i dy = 0 \quad (3.10)$$

Following the Galerkin weighted residual method and integration by parts method to the equations (3.8) – (3.10) we obtain

$$\int_{\eta_e}^{\eta_{e+1}} \frac{d\Psi_j^i}{dy} \frac{d\psi_j^i}{dy} dy - \delta M_1^2 \int_{\eta_e}^{\eta_{e+1}} u^i \Psi_j^i dy + \delta^2 A \int_{\eta_e}^{\eta_{e+1}} (u^i)^2 \Psi_j^i dy - \delta G \int_{\eta_e}^{\eta_{e+1}} (\theta^i + NC^i) \Psi_j^i dy = Q_{1,j} + Q_{2,j} \quad (3.11)$$

$$\text{where } -Q_{1,j} = \Psi_j(\eta_e) \frac{du^i}{d\eta}(\eta_e) \quad Q_{1,j} = \Psi_j(\eta_{e+1}) \frac{du^i}{d\eta}(\eta_{e+1})$$

$$\int_{\eta_e}^{\eta_{e+1}} \frac{d\Psi_j^i}{dy} \left(\frac{dC^i}{dy} \right) dy - (\gamma Sc) \int_{\eta_e}^{\eta_{e+1}} C^i \Psi_j^i dy + \frac{ScSo}{N} \int_{\eta_e}^{\eta_{e+1}} \frac{d\Psi_j^i}{dy} \left(\frac{d\theta^i}{dy} \right) \Psi_j^i dy - ScN_c \int_{\eta_e}^{\eta_{e+1}} u^i \Psi_j^i dy = R_{1,j} + R_{2,j} \quad (3.12)$$

$$\text{where } -R_{1,j} = \Psi_j(\eta_e) \frac{dC^i}{dy}(\eta_e) + \frac{ScSo}{N} \Psi_j(\eta_e) \frac{d\theta^i}{dy}(\eta_e)$$

$$R_{2,j} = \Psi_j(\eta_{e+1}) \left(\frac{dC^i}{dy}(\eta_{e+1}) + \frac{ScSo}{N} \frac{d\theta^i}{dy}(\eta_{e+1}) \right)$$

$$\int_{\eta_e}^{\eta_{e+1}} \frac{d\Psi_j^i}{dy} \frac{d\theta^i}{dy} dy - P_1 N_T \int_{\eta_e}^{\eta_{e+1}} u^i \Psi_j^i dy + Du N_2 \int_{\eta_e}^{\eta_{e+1}} \frac{d\Psi_j^i}{dy} \left(\frac{dC^i}{dy} \right) \Psi_j^i dy - \alpha_1 \int_{\eta_e}^{\eta_{e+1}} \theta^i dy = S_{1,j} + S_{2,j}$$

$$\text{where } -S_{1,j} = \Psi_j(\eta_e) \frac{d\theta^i}{dy}(\eta_e) + DuN_2 \Psi_j(\eta_e) \frac{dC^i}{dy}(\eta_e) \quad (3.13)$$

$$S_{2,j} = \Psi_j(\eta_{e+1}) \frac{d\theta^i}{dy}(\eta_{e+1}) + DuN_2 \Psi_j(\eta_{e+1}) \frac{dC^i}{dy}(\eta_{e+1})$$

Making use of equations (3.4) we can write above equations as

$$\sum_{k=1}^3 u_k \int_{\eta_e}^{\eta_{e+1}} \frac{d\psi_j^i}{dy} \frac{d\psi_k}{dy} dy - \sum_{k=1}^3 \delta M_1^2 u_k \int_{\eta_e}^{\eta_{e+1}} \psi_j^i \psi_k dy - \delta G \left(\sum_{k=1}^3 \theta_k \int_{\eta_e}^{\eta_{e+1}} \psi_j^i \psi_k dy + NC_k \sum_{k=1}^3 \psi_j^i \psi_k dy \right. \quad (3.14)$$

$$\left. + \delta^2 A \sum_{k=1}^3 u_k^2 \int_{\eta_e}^{\eta_{e+1}} \left(\frac{d\psi_k}{d\eta} \right)^2 \psi_j^i dy \right) = Q_{1,j} + Q_{2,j}$$

$$\sum_{k=1}^3 C_k \int_{\eta_e}^{\eta_{e+1}} \frac{d\psi_j^i}{dy} \frac{d\psi_k}{dy} dy - (\gamma Sc) \sum_{k=1}^3 C_k \int_{\eta_e}^{\eta_{e+1}} \psi_j^i \psi_k d\eta - ScN_c \sum_{k=1}^3 C_k \int_{\eta_e}^{\eta_{e+1}} \psi_j^i \psi_k dy \quad (3.15)$$

$$+ \frac{ScSo}{N} \sum_{k=1}^3 \theta_k \int_{\eta_e}^{\eta_{e+1}} \frac{d\psi_j^i}{dy} \frac{d\psi_k}{dy} dy = R_{1,j} + R_{2,j}$$

$$\sum_{k=1}^3 \theta_k \int_{\eta_e}^{\eta_{e+1}} \frac{d\psi_j^i}{dy} \frac{d\psi_k}{dy} dy - P_1 N_T \sum_{k=1}^3 u_k \int_{\eta_e}^{\eta_{e+1}} \psi_k \psi_j^i dy \quad (3.16)$$

$$+ DuN_2 \sum_{k=1}^3 C_k \int_{\eta_e}^{\eta_{e+1}} \frac{d\psi_j^i}{dy} \frac{d\psi_k}{dy} dy - \alpha_2 \sum_{k=1}^3 \theta_k \psi_k \psi_j^i dy = S_{1,j} + S_{2,j}$$

choosing different Ψ_j^i 's corresponding to each element η_e in the equation (3.14) yields a local stiffness matrix of order 3×3 in the form

$$(f_{i,j}^k)(u_i^k) - \delta G(g_{i,j}^k)(\theta_i^k + NC_i^k) + \delta D^{-1}(m_{i,j}^k)(u_i^k) + \delta^2 A(n_{i,j}^k)(u_i^k) = (Q_{i,j}^k) + (Q_{2,j}^k) \quad (3.17)$$

Likewise the equation (3.15) & (3.16) gives rise to stiffness matrices

$$(e_{i,j}^k)(C_i^k) + \frac{ScSo}{N}(t_{ij}^k)(\theta_i^k) - ScN_c(m_{i,j}^k)(u_i^k) = R_{1,j}^k + R_{2,j}^k \quad (3.18)$$

$$(l_{ij}^k)(\theta_i^k) - P_1 N_T(t_{ij}^k)(\theta_i^k) = S_{1,j}^k + S_{2,j}^k \quad (3.19)$$

where $(f_{i,j}^k), (g_{i,j}^k), (m_{i,j}^k), (n_{i,j}^k), (e_{i,j}^k), (t_{ij}^k)$ are 3×3 matrices and $(Q_{2,j}^k), (Q_{1,j}^k), (R_{2,j}^k), (R_{1,j}^k), (S_{2,j}^k)$ and $(S_{1,j}^k)$ are 3×1 column matrices and such stiffness matrices (3.17) – (3.19) in terms of local nodes in each element are assembled using inter element continuity and equilibrium conditions to obtain the coupled global matrices in terms of the global nodal values of k , θ & C . In case we choose n -quadratic elements then the global matrices are of order $2n+1$. The ultimate coupled global matrices are solved to determine the unknown global nodal values of the velocity, temperature and concentration in fluid region. In solving these global matrices an iteration procedure has been adopted to include the boundary and effects in the porous region.

The shape functions corresponding to

$$\begin{aligned} \Psi_1^1 &= \frac{(y-4)(y-8)}{32} & \Psi_2^1 &= \frac{(y-12)(y-16)}{32} & \Psi_3^1 &= \frac{(y-20)(y-24)}{32} \\ \Psi_1^2 &= \frac{(y-2)(y-4)}{8} & \Psi_2^2 &= \frac{(y-6)(y-8)}{8} & \Psi_3^2 &= \frac{(y-10)(y-12)}{8} \\ \Psi_1^3 &= \frac{(3y-4)(3y-8)}{32} & \Psi_2^3 &= \frac{(3y-12)(3y-16)}{32} & \Psi_3^3 &= \frac{(3y-20)(3y-24)}{32} \end{aligned}$$

$$\begin{aligned}\Psi_1^4 &= \frac{(y-1)(y-2)}{2} & \Psi_2^4 &= \frac{(y-3)(y-4)}{2} & \Psi_3^4 &= \frac{(y-5)(y-6)}{2} \\ \Psi_1^5 &= \frac{(5y-4)(5y-8)}{32} & \Psi_2^5 &= \frac{(5y-12)(5y-16)}{32} & \Psi_3^5 &= \frac{(5y-20)(5y-24)}{32}\end{aligned}$$

4. STIFFNESS MATRICES

The global matrix for θ is

$$A_3 X_3 = B_3 \quad (4.1)$$

The global matrix for N is

$$A_4 X_4 = B_4 \quad (4.2)$$

The global matrix u is

$$A_5 X_5 = B_5 \quad (4.3)$$

In fact, the non-linear term arises in the modified Brinkman linear momentum equation (3.8) of the porous medium. The iteration procedure in taking the global matrices as follows. We split the square term into a product term and keeping one of them say u_i 's under integration, the other is expanded in terms of local nodal values as in (3.4), resulting in the corresponding coefficient matrix (n_{ij}^k) in (3.17), whose coefficients involve the unknown u_i 's. To evaluated (3.18) to begin with choose the initial global nodal values of u_i 's as zeros in the zeroth approximation. We evaluate u_i 's, θ_i 's and C_i 's in the usual procedure mentioned earlier. Later choosing these values of u_i 's as first order approximation calculate θ_i 's, C_i 's. In the second iteration, we substitute for u_i 's the first order approximation of u_i 's and the first approximation of θ_i 's and C_i 's obtain second order approximation. This procedure is repeated till the consecutive values of u_i 's, θ_i 's and C_i 's differ by a preassigned percentage. For computational purpose we choose five elements in flow region.

5. SHEAR STRESS, NUSSELT NUMBER AND SHERWOOD NUMBER

The shear stress on the boundaries $y = \pm 1$ is given by $\tau_{y=\pm L} = \mu \left(\frac{du}{dy} \right)_{y=\pm L}$

The rate of heat transfer (Nusselt Number) is given by $Nu_{y=-1} = \left(\frac{d\theta}{dy} \right)_{y=-1}$

The rate of mass transfer (Sherwood Number) is given by $Sh_{y=-1} = \left(\frac{dC}{dy} \right)_{y=-1}$

6. DISCUSSION OF RESULTS

In this analysis we investigate the effect of soret and dufour effect on convective heat and mass transfer flow in a vertical channel with constant heat and mass flux. The equations governing the flow heat and mass transfer have been solved by employing Galerkin finite element analysis with quadratic approximation function.

The axial velocity u is shown in figs.1-3 for different values of G , M , D^{-1} , α , N , Sc , So , Du , K , N_1 and Q_1 . The actual axial flow in the vertical up word direction and hence $u < 0$ represents a reversal flow. With respect to Soret parameter So it can observed that the axial velocity reduces with increase in $So \leq 1.0$ and enhances with higher $So \geq 1.5$ (fig.4). With respect to Dufour parameter Du we notice an enhancement in $|u|$ with increase in Du (fig.1). The effect of chemical reaction parameter K on u is shown in fig.2. It is found that the axial velocity reduces with increase in chemical reaction parameter $K \leq 1.5$ and enhances with higher $K \geq 2.5$ in the degenerating chemical reaction case while in generating chemical reaction case it enhances in the flow region. Fig.3 represents u with Thermal radiation N_1 and Radiation absorption parameter Q_1 . We find an enhancement in $|u|$ with increase in radiation parameter N_1 . With respect to Q_1 it can be seen that $|u|$ enhances with increase in $Q_1 \leq 1.5$ and reduces with higher $Q_1 \geq 2.5$.

The non-dimensional temperature θ is shown in figs.4-6 for different parametric values. It is found that the actual temperature (T) enhances with increase in $|G|$. An increase in So leads to an enhancement in actual temperature while it reduces with increase in Du (fig.4). Fig.5 represents the variation of θ with chemical reaction parameter K it can be seen from the profiles that the actual temperature depreciates in the degenerating chemical reaction case and enhances in the generating chemical reaction case. The variation of θ with radiation parameter N_1 indicates that higher the thermal radiative heat flux smaller the actual temperature. An increase in radiation absorption parameter Q_1 leads to an enhancement in actual temperature (fig.6).

The non-dimensional concentration C is shown in figs.7-9 for different parametric values. Fig.7 represents the concentration with So and Du . It is found that an increase in So reduces the concentration while it enhances with increase in Du . Fig.8 represents C with chemical reaction parameter K . It is found that the concentration reduces in degenerating chemical reaction case and enhances in the generating chemical reaction case. With respect to radiation parameter N_1 we find that higher the radiative heat flux ($N_1 \leq 3.5$) smaller the concentration and for further higher values of $N_1 \geq 5$ larger the concentration. Also the concentration experiences an enhancement with increase in radiation absorption parameter Q_1 (fig.9).

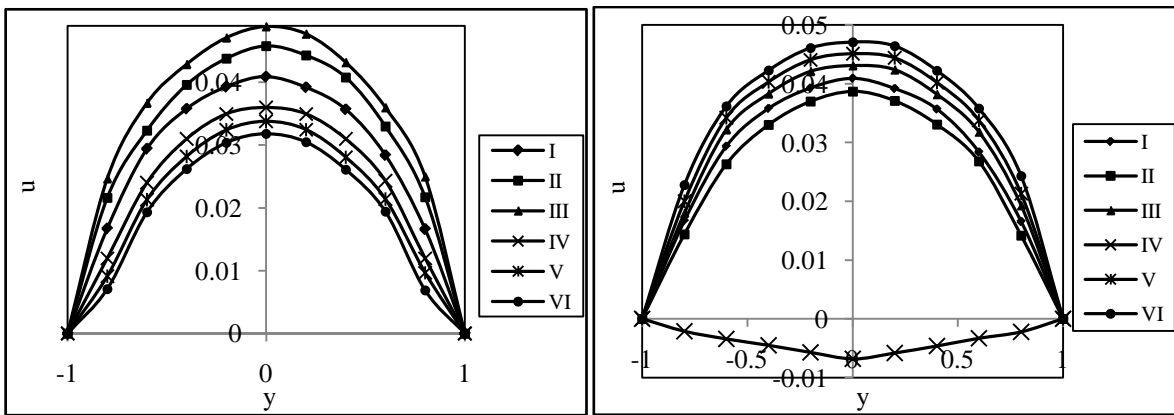


Figure-1: Variation of u with Du and So

	I	II	III	IV	V	VI
Du	0.01	0.03	0.05	0.01	0.01	0.01
So	0.5	0.5	0.5	1	1.5	2.5

Figure-2: Variation of u with K

	I	II	III	IV	V	VI
K	0.5	1.5	2.5	-0.5	-1.5	-2.5

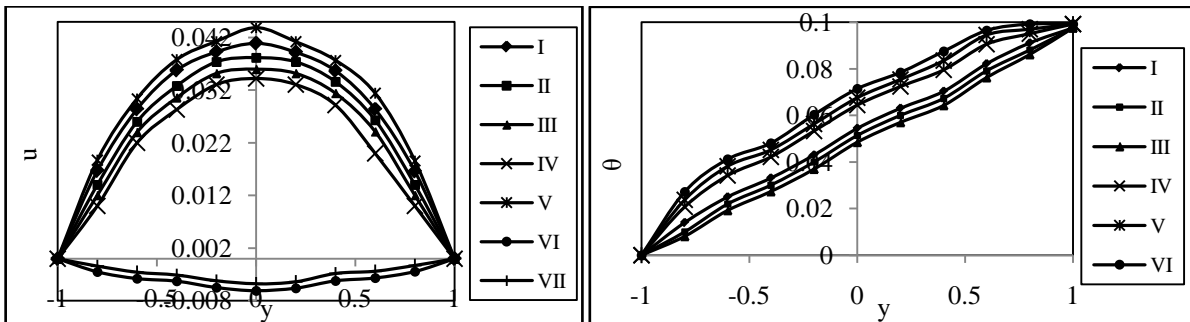


Figure-3: Variation of u with N_1 and Q_1

	I	II	III	IV	V	VI	VII
N_1	1.5	3.5	5	10	1.5	1.5	1.5
Q_1	0.5	0.5	0.5	0.5	1.5	2.5	3.5

Figure-4: Variation of θ with Du and So

	I	II	III	IV	V	VI
Du	0.01	0.03	0.05	0.01	0.01	0.01
So	0.5	0.5	0.5	1	1.5	2.5

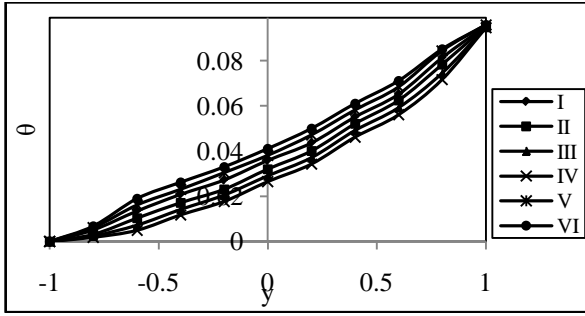


Figure-5: Variation of θ with K

	I	II	III	IV	V	VI
K	0.5	1.5	2.5	-0.5	-1.5	-2.5

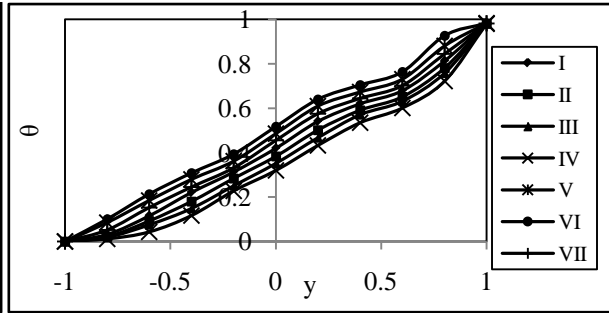


Figure-6: Variation of θ with N_1 and Q_1

	I	II	III	IV	V	VI	VII
N_1	1.5	3.5	5	10	1.5	1.5	1.5
Q_1	0.5	0.5	0.5	0.5	1.5	2.5	3.5

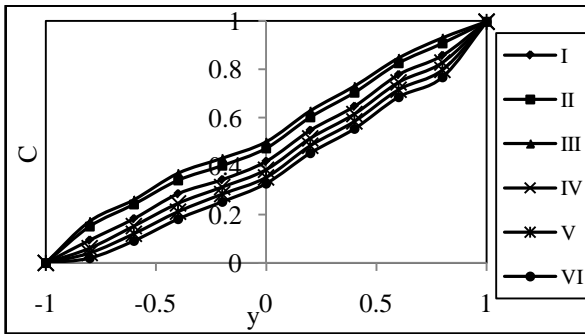


Figure-7: Variation of C with Du and So

	I	II	III	IV	V	VI
Du	0.01	0.03	0.05	0.01	0.01	0.01
So	0.5	0.5	0.5	1	1.5	2.5

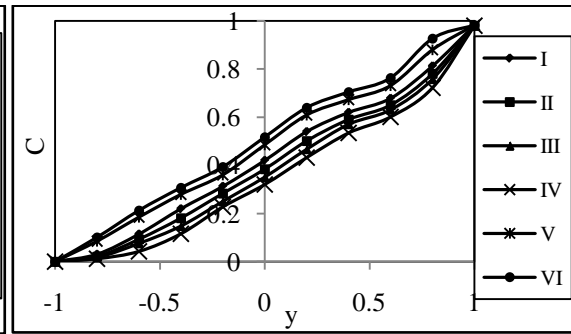


Figure-8: Variation of C with K

	I	II	III	IV	V	VI
K	0.5	1.5	2.5	-0.5	-1.5	-2.5

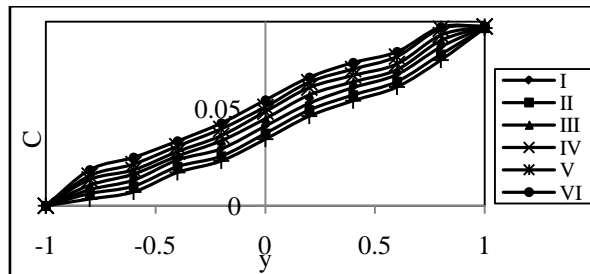


Figure-9: Variation of C with N_1 and Q_1

	I	II	III	IV	V	VI	VII
N_1	1.5	3.5	5	10	1.5	1.5	1.5
Q_1	0.5	0.5	0.5	0.5	1.5	2.5	3.5

Table-1: Shear stress (τ) at $y=+1$

G	I	II	III	IV	V	VI	VII
10^3	0.0228	0.0217	0.0197	0.0159	0.1273	0.1475	0.1879
3×10^3	0.0215	0.0189	0.0176	0.0163	0.2013	0.2362	0.2912
-10^3	0.0222	0.0161	0.0144	0.0126	0.0355	0.0550	0.0876
-3×10^3	0.0243	0.0228	0.0210	0.0170	0.7037	0.7202	0.8428
So	0.5	1	1.5	2.5	0.5	0.5	0.5
Du	0.01	0.01	0.01	0.01	0.03	0.05	0.07

Table-2: Shear stress (τ) at $y = -1$

G	I	II	III	IV	V	VI	VII
10^3	-0.0983	-0.0995	-0.1257	-0.1268	-0.0913	-0.0903	-0.0883
3×10^3	-0.0940	-0.0968	-0.0975	-0.1081	-0.0927	-0.0890	-0.0574
-10^3	-0.0544	-0.0578	-0.1087	-0.1092	-0.0519	-0.0430	-0.0314
-3×10^3	-0.0841	-0.0874	-0.1267	-0.1360	-0.0815	-0.0344	-0.0316
So	0.5	1	1.5	2.5	0.5	0.5	0.5
Du	0.01	0.01	0.01	0.01	0.03	0.05	0.07

Table-3: Shear stress (τ) at $y = +1$

G	I	II	III	IV
10^3	0.0221	0.0228	0.011	0.0317
3×10^3	0.0150	0.0172	0.0114	0.0284
-10^3	0.0256	0.0269	0.0241	0.0357
-3×10^3	0.0473	0.0577	0.0452	0.0666
N_1	1.5	3.5	5	10

Table-4: Shear stress (τ) at $y = -1$

G	I	II	III	IV
10^3	-0.1106	-0.1289	-0.1067	-0.0916
3×10^3	-0.0726	-0.0791	-0.0701	-0.0698
-10^3	-0.1074	-0.1087	-0.1010	-0.0965
-3×10^3	-0.1044	-0.1114	-0.1032	-0.0865
N_1	1.5	3.5	5	10

Table-5: Shear stress (τ) at $y = +1$

G	I	II	III	IV	V	VI	VII	VIII	IX	X
10^3	0.2011	0.1322	0.1370	-0.0437	0.0262	0.1175	0.3083	0.6615	0.1148	0.1061
3×10^3	0.4274	0.1977	0.2198	-0.8204	-0.5589	0.0620	0.4604	0.4867	-0.0147	-0.2739
-10^3	0.0541	0.0182	0.1165	-0.1906	0.1322	0.1370	0.2307	0.2983	-3.0438	-5.9606
-3×10^3	0.1052	0.0504	0.1844	-0.3287	0.1250	0.1336	0.2046	0.3412	-6.1662	-11.0626
K	0.5	1.5	2.5	-0.5	-1.5	-2.5	0.5	0.5	0.5	0.5
Q_1	0.25	0.25	0.25	0.25	0.25	0.25	0.5	1	1.5	2.5

Table-6: Shear stress (τ) at $y = -1$

G	I	II	III	IV	V	VI	VII	VIII	IX	X
10^3	-3.2867	-0.1305	-0.1141	-2.0499	-9.0662	-9.7517	-1.4607	0.6615	0.7123	1.0487
3×10^3	-1.8301	-0.3178	-0.1026	-3.2156	-3.7763	-4.2209	-1.9033	0.4867	1.4680	1.6548
-10^3	-2.3210	-0.9203	-0.4161	-0.4975	-1.3068	-1.5418	-2.6456	0.1983	1.3171	1.5599
-3×10^3	-4.5032	-2.2198	-0.0928	-0.2031	-1.1448	-1.3542	-4.9088	0.3412	1.4761	1.7820
K	0.5	1.5	2.5	-0.5	-1.5	-2.5	0.5	0.5	0.5	0.5
Q_1	0.25	0.25	0.25	0.25	0.25	0.25	0.5	1	1.5	2.5

Table-7: Nusselt number (Nu) at $y = -1$

G	I	II	III	IV	V	VI	VII
10^3	0.0107	0.0448	0.0455	0.0471	0.0192	0.0182	0.0171
3×10^3	0.0102	0.0398	0.0416	0.0434	0.0095	0.0085	0.0074
-10^3	0.0124	0.0575	0.0590	0.0622	0.0113	0.0103	0.0099
-3×10^3	0.0111	0.0616	0.0653	0.0703	0.0097	0.0087	0.0077
So	0.5	1	1.5	2.5	0.5	0.5	0.5
Du	0.01	0.01	0.01	0.01	0.03	0.05	0.07

Table-8: Nusselt number (Nu) at y= -1

G	I	II	III	IV
10^3	0.0442	0.0452	0.0322	0.0246
3×10^3	0.0366	0.0375	0.0321	0.0264
-10^3	0.0515	0.0528	0.0493	0.0223
-3×10^3	0.0318	0.0474	0.0292	0.0122
N_1	1.5	3.5	5	10

Table-9: Nusselt number (Nu) at y= -1

G	I	II	III	IV	V	VI	VII	VIII	IX	X
10^3	0.7522	0.1919	0.1580	-0.0928	-0.0764	-0.0707	0.7638	0.6615	0.6148	0.5548
3×10^3	0.5121	0.3083	0.0996	-0.7881	-0.7249	-0.0801	0.5255	0.4867	0.3915	0.3438
-10^3	0.2003	0.1109	0.1026	-0.5298	-0.5021	-0.0477	0.2144	0.1983	0.1849	0.1622
-3×10^3	0.3427	0.2747	0.2487	-0.5210	-0.5067	-0.0447	0.3779	0.3412	0.3081	0.2386
K	0.5	1.5	2.5	-0.5	-1.5	-2.5	0.5	0.5	0.5	0.5
Q_1	0.25	0.25	0.25	0.25	0.25	0.25	0.5	1	1.5	2.5

Table-10: Sherwood Number (Sh) at y= -1

G	I	II	III	IV	V	IV	VII
10^3	0.0831	0.0416	0.0409	0.0386	0.1738	0.1756	0.2269
3×10^3	0.0792	0.0368	0.0359	0.0308	0.8853	0.9658	0.9691
-10^3	0.0737	0.0699	0.0689	0.0559	0.1859	0.3288	0.4105
-3×10^3	0.0869	0.0567	0.0552	0.0467	0.6617	0.9750	0.9957
So	0.5	1	1.5	2.5	0.5	0.5	0.5
Du	0.01	0.01	0.01	0.01	0.01	0.01	0.01

Table-11: Sherwood Number (Sh) at y= -1

G	I	II	III	IV
10^3	0.0427	0.0467	0.0643	0.0681
3×10^3	0.0351	0.0361	0.0505	0.0523
-10^3	0.0498	0.0509	0.0761	0.0804
-3×10^3	0.0278	0.0577	0.0683	0.0716
N_1	1.5	2.5	5	10

Table-12: Sherwood Number (Sh) at y= -1

G	I	II	III	IV	V	VI	VII	VIII	IX	X
10^3	0.6643	0.1280	0.0735	-0.3113	-0.1050	-0.0962	0.7046	0.6615	0.5458	0.4297
3×10^3	0.8905	0.1805	0.0610	-0.2380	-0.1958	-0.1888	0.9911	0.8867	0.8219	0.7346
-10^3	0.2761	0.1918	0.1445	-0.7688	-0.1846	-0.1434	0.3495	0.2983	0.2542	0.2165
-3×10^3	0.4983	0.4805	0.1728	-0.7072	-0.1652	-0.1266	0.8512	0.7412	0.6426	0.5344
K	0.5	1.5	2.5	-0.5	-1.5	-2.5	0.5	0.5	0.5	0.5
Q_1	0.25	0.25	0.25	0.25	0.25	0.25	0.5	1	1.5	2.5

The shear stress τ at the boundaries $y = \pm 1$ is shown in tables 1-6 for different values $G, M, D^{-1}, \alpha, N, Sc, So, Du, K, N_1$ and Q_1 . It is found that the shear stress τ enhances with increase in $G > 0$ on both the walls. While an increase in $|G| (< 0)$ reduces $|\tau|$ on $y = -1$ and enhances on $y = +1$. An increase in So (decrease in Du) leads to a depreciation in $|\tau|$ on both the walls (tables.1&2). Tables.3&4 represents the stress with radiation parameter N_1 . It is found that the stress on $y = +1$ enhances with increase in ($N_1 \leq 3.5$), reduces with higher $N_1 = 5$ and again enhances with still higher $N_1 = 10$. On $y = -1$, $|\tau|$ enhances with $N_1 \leq 3.5$ and reduces with higher $N_1 \geq 5$. The variation of τ with chemical reaction parameter K shows that the stress at $y = +1$ reduces with $|K| \leq 1.5$ and enhances with higher $|K| \geq 2.5$ while on $y = -1$, $|\tau|$ reduces in the degenerating chemical reaction case and enhances in generating chemical reaction case. An increase in the radiation absorption parameter $Q_1 \leq 1$ enhances $|\tau|$ and reduces with higher $Q_1 \geq 1.5$ on $y = +1$. While on $y = -1$, $|\tau|$ reduces with $Q_1 \leq 0.5$ and enhances with higher $Q_1 \geq 1.5$ (tables.5&6).

The rate of heat transfer (Nusselt number (Nu)) on the wall $y=-1$ is exhibited in the tables 7-9 for different parametric values. It is found that the rate heat transfer on $y=-1$ reduces with increase in $G>0$ and enhances with $G<0$. Table.10 represents Nu with Sc, So and Du. It is found that lesser the molecular diffusivity larger the rate of heat transfers. Increasing the Soret parameter So (decreasing Du) leads to an enhancement in the rate of heat transfer on $y=-1$ (table.7). Table.8 represents Nu with radiation parameter N_1 . It can be observed that the Nusselt number enhances with $N_1 \leq 3.5$ and reduces with $N_1 \geq 5$. The rate of heat transfer reduces on $y=-1$ in both degenerating and generating chemical reaction cases. An increase in $Q_1 \leq 0.5$ leads to an enhancement in $|Nu|$ and reduces for higher $Q_1 \geq 1$ (table.9).

The rate of mass transfer (Sherwood Number (Sh)) on $y=-1$ is shown in tables.10-12 for different parametric values. From table.10 an increasing So (decreasing Du) results an enhancement in $|Sh|$ on $y=-1$. The variation of Sh with N_1 shows that higher the radiative heat flux larger the rate of mass transfer on $y=-1$ (table.11). From table.12 we find that the rate of mass transfer reduces in both degenerating and generating chemical reaction cases. An increase in $Q_1 \leq 0.5$ enhances $|Sh|$ and for higher $Q_1 \geq 1$ we find a depreciation in $|Sh|$ on $y=-1$.

7. CONCLUSIONS

- (i) With respect to Soret parameter So it can observed that the axial velocity reduces with increase in $So \leq 1.0$ and enhances with higher $So \geq 1.5$. With respect to Dufour parameter Du we notice an enhancement in $|u|$ with increase in Du. An increase in So leads to an enhancement in actual temperature while it reduces with increase in Du. The concentration with So and Du. It is found that an increase in So reduces the concentration while it enhances with increase in Du.
- (ii) The effect of chemical reaction parameter K on u is shown in fig.5. It is found that the axial velocity reduces with increase in chemical reaction parameter $K \leq 1.5$ and enhances with higher $K \geq 2.5$ in the degenerating chemical reaction case while in generating chemical reaction case it enhances in the flow region. The variation of θ with chemical reaction parameter K it can be seen from the profiles that the actual temperature depreciates in the degenerating chemical reaction case and enhances in the generating chemical reaction case. It is found that the concentration reduces in degenerating chemical reaction case and enhances in the generating chemical reaction case.
- (iii) We find an enhancement in $|u|$ with increase in radiation parameter N_1 . The variation of θ with radiation parameter N_1 indicates that higher the thermal radiative heat flux smaller the actual temperature. With respect to radiation parameter N_1 we find that higher the radiative heat flux ($N_1 \leq 3.5$) smaller the concentration and for further higher values of $N_1 \geq 5$ larger the concentration.
- (iv) With respect to Q_1 it can be seen that $|u|$ enhances with increase in $Q_1 \leq 1.5$ and reduces with higher $Q_1 \geq 2.5$. An increase in radiation absorption parameter Q_1 leads to an enhancement in actual temperature. With respect to Q_1 the concentration experiences an enhancement with increase in radiation absorption parameter Q_1 .

8. REFERENCE

1. Cheng P. Heat transfer in geothermal systems. Adv. Heat transfer 1978; 14:1-105.
2. Prasad V, Tuntomo A. Inertia Effects on Natural Convection in a vertical porous cavity, numerical Heat Transfer 1987;11:295-320.
3. Vafai K, Tien CL. Boundary and Inertia effects on flow and Heat Transfer in Porous Media, Int. J. Heat Mass Transfer, 1981; 24:195-203.
4. Vafai K, Thyagaraju R. Analysis of flow and heat Transfer at the interface region of a porous medium, Int. J. Heat Mass Trans 1987; 30:1391-1405
5. Tien D, CV, Hong JT. Natural convection in porous media under non-Darcian and non-uniform permeability conditions, hemisphere, Washington.C; 1985.
6. [6]. Prasad V, KulackiFA, keyhani M. Natural convection in a porous medium" J.Fluid Mech. 1985; 150: 89-119.
7. Kalidas N,Prasad V. Benard convection in porous media Effects of Darcy and Pransdtl Numbers, Int. Syms. Convection in porous media, non-Darcy effects, proc.25th Nat. Heat Transfer Conf. 1988; 1:593-604.

8. Poulikakos D, Bejan A. The Departure from Darcy flow in Nat. Convection in a vertical porous layer, physics fluids 1985; 28:3477-3484.
9. Tong TL, Subramanian E. A boundary layer analysis for natural convection in porous enclosures: use of the Brinkman-extended Darcy model, Int.J.Heat Mass Transfer.1985;28:563-571.
10. Laurait G, PrasadV. Natural convection in a vertical porous cavity a numerical study of Brinkman extended Darcy formulation. J.Heat Transfer.1987; 295-320.
11. Beckermann C, VisakantaR, Ramadhyani S. A numerical study of non-Darcian natural convection in a vertical enclosure filled with a porous medium. Numerical Heat transfer 1986; 10:557-570.
12. El.Hakim MA. MHD oscillatory flow on free convection radiation through a porous medium with constant suction velocity, J.mason.Mater, 2000; 220: 271-276.
13. Jha BK, Singh A K.Soret effects on free-convection and mass transfer flow in the stokes problem for a infinite vertical plate. Astrophys. Space Sci.1990; 173(2):251-255(1990).
14. Kafousia NG,Astrophys. Space Sci.1990; 173:251.
15. AbdulSattar Md, Alam Md. Thermal diffusion as well as transprotaion effect on MHD free convection and Mass Transfer flow past an accelerated vertical porous plate, Ind Journal of Pure and Applied Maths.1995; 24: 679-688.
16. Malasetty MS, Gaikwad SN. Effect of cross diffusion on double diffusive convection in the presence of horizontal gradient,Int.Journal Eng.Science, 2002;40:773-787.
17. Bharathi K. Convective heat and mass transferthrough a porous medium in channels / pipes with radiation and soret effects, Ph.D. Thesis, S.K.University, Anantapur, A.P., India, 2007
18. Taneja, Rajeev, Jain NC. Effect of magnetic field on free convection mass transfer flow through porous medium with radiation and variable permeability in slip flow regime., Janabha,2002;31/32,69.
19. Kumar A, Singh NP, Singh AK, Kumar H. MHD free convection flow of a viscous fluid past a porous vertical plate through non-homogeneous porous medium with radiation and temperature gradient dependent heat source in slip glow regime, Ultra Sci.Phys.Sci (India) 2006;8:39-46.
20. Makinde OD. Free convection flow with thermal radiation and mass transfer pass a moving vertical porous plate, Int.Commun.Heat and Mass transfer (U.K) 2005; 32:1411-1419.
21. Ayani MB, Fsfahani JH. The effect of radiation on the natural convection induced by a line heat source.Int.J.Nummer.Method,Heat fluid flow (U.K.),2006;16:28-45.
22. Raphil A. Radiation and free convection flow through a porous medium, Int.Commun.Heat and Mass transfer, 1998; 25:289-295.
23. Nagaleelakumari.S. Combined influence of chemical reaction and Soret effect on hydrodynamic non-Darcy convective heat and mass transfer flow through a porous medium in a vertical channel with heat generating sources, Ph.D thesis, SP Mahila University, Tirupati, AP-India, 2012.
24. Muralidhar.P. Effect of chemical reaction and thermo diffusion on convective heat and mass transfer flow of viscous fluid through a porous medium in a vertical channel, Ph.D thesis, Andhra University, Vishakapatnam, AP-India, 2012.

Source of support: Nil, Conflict of interest: None Declared.

[Copy right © 2017. This is an Open Access article distributed under the terms of the International Journal of Mathematical Archive (IJMA), which permits unrestricted use, distribution, and reproduction in any medium, provided the original work is properly cited.]